

---

# Quantitation of Iodine-123- $\beta$ -CIT Dopamine Receptor Uptake in a Phantom Model

L.K. Leong, M.K. O'Connor and D.M. Maraganore

Departments of Radiology and Neurology, Mayo Clinic, Rochester, Minnesota

---

**Objective:** The purpose of this study was to determine the effects of technical factors such as collimation and filtration on the measurement of  $^{123}\text{I}$ - $\beta$ -CIT uptake in the striatum.

**Methods:** All SPECT studies were performed using a brain phantom containing striata within a bone- and tissue-equivalent skull. The effects of collimator resolution and septal penetration were assessed from  $^{99\text{m}}\text{Tc}$  and  $^{123}\text{I}$  studies containing variable activities in the striata and background regions. Optimum attenuation coefficients ( $\mu$ ) were determined from studies containing uniform activity in the brain.

**Results:** For  $^{99\text{m}}\text{Tc}$ ,  $\mu$  was  $0.095\text{ cm}^{-1}$  and  $0.07\text{ cm}^{-1}$  for parallel-hole and fanbeam collimators, respectively. For  $^{123}\text{I}$ , these values dropped to  $0.09\text{ cm}^{-1}$  and  $0.00\text{ cm}^{-1}$  (zero) for medium-energy and fanbeam collimators, respectively. Striatal uptake was significantly underestimated, particularly for medium-energy and general-purpose collimators. With  $^{99\text{m}}\text{Tc}$ , fanbeam collimation gave a 50% increase in the measured striatal uptake, compared to medium-energy collimation. However, with  $^{123}\text{I}$ , this gain was eliminated by septal penetration and scatter. Increasing transaxial slice thickness, ROI size and decreasing filter cutoff frequency all degraded apparent striatal uptake.

**Conclusion:** Partial volume effects, combined with the averaging effects of increasing slice thickness and ROI size, are the most significant factors affecting measurement of striatal uptake of  $^{123}\text{I}$ - $\beta$ -CIT. The increased resolution of low-energy high-resolution collimators, compared to a medium-energy collimator, is offset by the increased septal penetration and scatter.

**Key Words:** iodine-123- $\beta$ -CIT; dopamine receptors; SPECT; brain phantom

*J Nucl Med Technol* 1999; 27:117-122

---

Alteration of the dopamine or serotonin systems has been thought to play a key role in the pathogenesis of several neuropsychiatric disorders (1,2). A decrease in the dopamine neurons in the striatum is the major pathological change of Parkinson's disease. Iodine-123- $\beta$ -CIT ( $^{123}\text{I}$ -labeled 2 $\beta$ -carboxymethoxy-3 $\beta$ -4iodophenyl tropane) is an analog of

cocaine that has been shown to have a high affinity for the dopamine and serotonin transport sites in the brain (3-5). SPECT studies using  $^{123}\text{I}$ - $\beta$ -CIT have shown that a reduction in the striatal uptake of this radiopharmaceutical correlates with the severity of Parkinson's disease (6). Relative striatal uptake of  $^{123}\text{I}$ - $\beta$ -CIT generally has been estimated from region of interest (ROI) analysis of the tomographic slices, however, published studies have used different regions of the striatum for estimating uptake (6-8). Furthermore, no consensus exists as to the optimal acquisition and processing parameters for such studies. As a consequence, reported uptake values of  $^{123}\text{I}$ - $\beta$ -CIT in the striata of normal subjects have shown wide variation between different laboratories (9).

Quantitation of  $^{123}\text{I}$ - $\beta$ -CIT uptake in the brain is complicated by several technical factors. These include imaging factors, such as the amount of scatter present, type of collimation used, and processing parameters such as filtration and attenuation correction. Finally, results will depend on analytical parameters, such as slice thickness and ROI size and placement. Failure to optimize these parameters will make it difficult to compare results between different laboratories and may reduce the overall sensitivity of the technique to small changes in dopamine receptor uptake in the brain. The purpose of this study was to evaluate the effects of these parameters on quantitative indices of  $^{123}\text{I}$ - $\beta$ -CIT uptake in a phantom model of the brain. This evaluation should provide guidelines as to the significance of these parameters on accurate quantitation of receptor uptake of  $^{123}\text{I}$ - $\beta$ -CIT.

## MATERIALS AND METHODS

All phantom studies were performed using a striatal head phantom (Radiology Support Devices, Long Beach, CA). This phantom contains a brain compartment with separate compartments for left and right caudate and left and right putamen. A bone-equivalent material is used to simulate the skull and a plastic material is used to simulate soft tissue of the head and neck, permitting the phantom to accurately simulate the attenuation characteristics of a normal head (10). Images of the head phantom containing either  $^{99\text{m}}\text{Tc}$  or  $^{123}\text{I}$  were acquired on a dual-head gamma-camera system. The following acquisition parameters were used for all studies:  $128 \times 128$  matrix; 120 views/head; 10-30 s/view; radius of rotation = 13 cm. Energy

---

For correspondence or reprints contact: Dr. Michael K. O'Connor, Section of Nuclear Medicine, Charlton 2N-213, Mayo Clinic, Rochester, MN 55905.

windows were set at 20% and were centered around the 140-keV and the 159-keV photopeaks of  $^{99m}\text{Tc}$  and  $^{123}\text{I}$ , respectively. A zoom factor of 2 was used for all studies using parallel-hole collimation, and a zoom factor of 1 for studies using fanbeam collimation.

#### Attenuation Correction

The brain and striatal compartments of the head phantom were filled with a uniform concentration of either  $^{99m}\text{Tc}$  or  $^{123}\text{I}$  to determine the optimum values of attenuation coefficients for tomographic studies of the head. Tomographic acquisitions were performed as described above using either a medium-energy collimator (MEGP) or a low-energy ultra-high resolution fanbeam collimator (UHRFB). Tomographic images were reconstructed using a Butterworth filter, order 5, with cutoff at 0.4 Nyquist. Attenuation correction was performed on the reconstructed transaxial slices using Chang's method (11). Values of the attenuation coefficient varied between  $0.0\text{ cm}^{-1}$  and  $0.15\text{ cm}^{-1}$ . Optimum values of the attenuation coefficient were determined by placing an irregular ROI around activity in a 1.76-cm thick transaxial slice of the midbrain (Fig. 1A) and determining the coefficient of variation (SD/mean) of counts within the region (10). The effect of variations in the attenuation coefficient on the measurement of relative striatal uptake was determined from analysis of  $^{123}\text{I}$  transaxial slices acquired with the MEGP and UHRFB collimators, as described in the sections on septal penetration and filtration below.

#### Collimator Resolution

Four different collimators were evaluated to determine the effect of collimator resolution on measurement of relative striatal uptake. For each collimator, a  $^{99m}\text{Tc}$  point source was placed at the center of rotation. A tomographic study was acquired and reconstructed in an identical manner to the phantom studies (i.e., same radius of rotation, matrix size, zoom factor and reconstruction filter). The tomographic resolution of each collimator was determined from measurement of the full width at half maximum (FWHM) of a profile drawn through the point source. Table 1 describes the collimator characteristics and their corresponding resolutions.

The effect of collimator resolution on the quantitation of striatal uptake was determined by imaging the striatal phantom with the 4 collimators described in Table 1. For this part of the

**TABLE 1**  
Description of the 4 Collimators Used  
in this Study\*

Collimator	System resolution		System sensitivity (cts/min/ $\mu\text{Ci}$ )†
	Measured in air at 13 cm	Measured in air at 10 cm†	
MEGP	10.9 mm	9.4 mm	160
LEGP	10.4 mm	9.0 mm	270
LEHR	7.8 mm	7.4 mm	160
UHRFB	6.6 mm	6.6 mm	220

\*System resolution was measured at the same radius of rotation (13 cm) as used for all the phantom studies.

†Values are taken from manufacturer's specifications for these collimators.

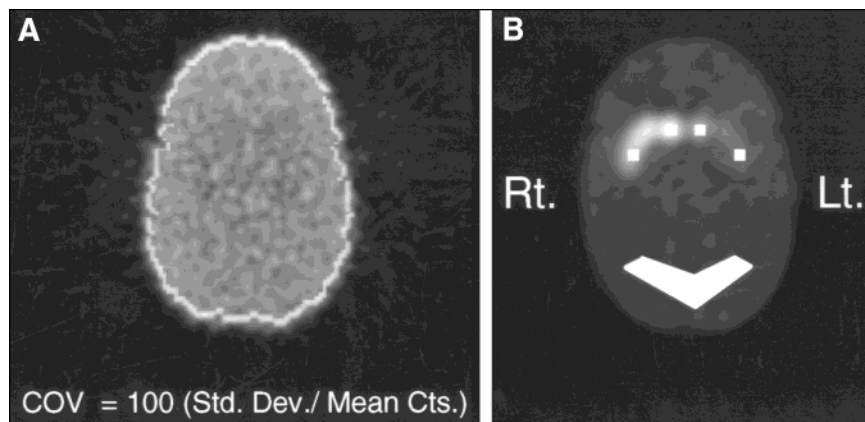
MEGP = medium-energy, general purpose; LEGP = low-energy, general purpose; LEHR = low-energy, high-resolution; UHRFB = low-energy, ultra-high resolution fan beam.

study,  $^{99m}\text{Tc}$  was used rather than  $^{123}\text{I}$  to eliminate the confusing effects of septal penetration in the low-energy collimators. The following concentrations of  $^{99m}\text{Tc}$  were used in the striatal phantom: background = 0.37 MBq/mL; right caudate = 3.7 MBq/mL; right putamen = 2.78 MBq/mL; left caudate = 1.85 MBq/mL; left putamen = 0.93 MBq/mL. Tomographic images of the striatal phantom were acquired and reconstructed as described above. Attenuation correction was applied to all studies based on the optimum values for the attenuation coefficients derived in the section on attenuation correction above. Quantitation of relative striatal uptake was determined from a 1.76-cm thick transaxial slice. Small  $4 \times 4\text{-mm}$  ROIs were placed over the caudate and putamen and a background ROI, representing nonstriatal uptake, was placed over the occipital lobe region (Fig. 2). See the section on ROI analysis below for complete details of quantitation of relative striatal uptake.

#### Septal Penetration

To determine the effects of septal penetration on quantitative analysis of relative striatal activity, images of the striatal phantom containing  $^{123}\text{I}$  were acquired using the MEGP collimator and the UHRFB collimator. For each collimator, a series of 5

**FIGURE 1.** (A) Transaxial slice through midsection of the brain phantom uniformly filled with  $^{99m}\text{Tc}$ . Coefficient of variation (COV) of counts within the brain determined from an irregular ROI placed around brain activity. (B) Transaxial slice through midsection of the brain phantom containing various concentrations of  $^{99m}\text{Tc}$  as described in Methods. Small  $4 \times 4\text{-mm}$  ROIs are shown over each caudate and putamen and a large ROI is drawn over the occipital region.



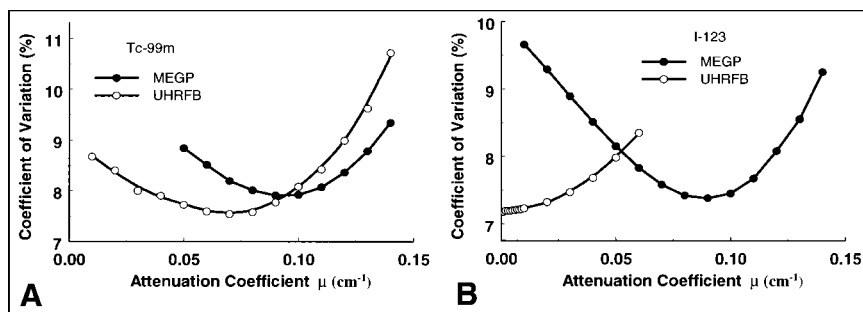


**FIGURE 2.** Coefficient of variation of counts within a uniformly filled brain phantom for the medium-energy (MEGP) and ultra-high resolution fanbeam (UHRFB) collimators as a function of the attenuation coefficient for (A)  $^{99m}\text{Tc}$  and (B)  $^{123}\text{I}$ .

acquisitions was performed. Table 2 describes the relative concentrations of  $^{123}\text{I}$  placed in the background compartment and in the left and right striatal compartments for each of the 5 acquisitions. Quantitation of relative striatal uptake was determined as described in the section on ROI analysis below.

#### Filtration

SPECT reconstruction usually uses a smoothing filter to reduce image noise. Previous studies with  $^{123}\text{I}$ - $\beta$ -CIT have used a Butterworth filter, with order 5–10 and cutoff between  $0.5\text{ cm}^{-1}$  and  $1.0\text{ cm}^{-1}$  (5,6,12). We reconstructed the planar data acquired with the UHRFB collimator (see section on collimator resolution above) using a Butterworth filter with a range of cutoff frequencies between  $0.2\text{ cm}^{-1}$  and  $2.0\text{ cm}^{-1}$  and an order in the range 5–10. Quantitation of relative striatal uptake was determined as described in the section on ROI analysis below.

#### Slice Selection

The effect of slice thickness on relative striatal uptake was determined from analysis of the reconstructed transaxial data acquired with  $^{99m}\text{Tc}$  for the 4 collimators described in the section on collimator resolution above. Reconstructed slice thickness was 2.2 mm (4.4 mm for UHRFB). One- to 10-pixel thick slices were produced with slice thickness of between 2.2 and 22 mm, respectively. Criteria for slice selection were as follows:

- 1 pixel thick: slice containing highest counts in striata;
- 2 pixels thick: 2 slices containing the highest counts in striata;

**TABLE 2**  
Relative Concentrations of Iodine-123 Used in the Brain Phantom to Compare MEGP and UHRFB Collimators

Acquisition number	Left striatum activity (kBq)	Right striatum activity (kBq)	Background activity (kBq)
1	370	2220	370
2	740	2590	370
3	1110	2960	370
4	1480	3330	370
5	1850	3700	370

- 3 pixels thick: slice containing highest counts in striata + 1 slice superior and 1 slice inferior to it; and
- 4–10 pixels thick: as above with successive addition of slices demonstrating decreasing striatal activity.

Quantitation of relative striatal uptake was determined as described in the section on ROI analysis below.

#### Region of Interest Analysis

For estimation of relative uptake in the caudate and putamen, square ROIs were placed over the caudate and putamen regions (Fig. 1B). For the caudate region, the ROI was placed over the caudate and adjusted to yield the maximum average counts per pixel. The putamen ROI was initially placed 1 cm inferior to the caudate ROI. The putamen ROI then was shifted laterally until the region of highest activity was obtained. ROI size was varied from  $1 \times 1$  pixel ( $2 \times 2\text{ mm}$ ) to  $5 \times 5$  pixels ( $10 \times 10\text{ mm}$ ). A background region was drawn over the occipital region. The caudate- or putamen-to-occipital ratio was calculated from the average counts per pixel in the caudate or putamen ROI divided by the average counts per pixel in the occipital ROI. Caudate-to-putamen ratios were calculated in a similar manner. Unless otherwise stated, all results refer to analysis of 1.76-cm transaxial slices acquired with  $^{99m}\text{Tc}$  and an ROI of  $4 \times 4\text{-mm}$  dimensions.

## RESULTS

Figure 2A plots the coefficient of variation of counts within the brain as a function of the attenuation coefficient for  $^{99m}\text{Tc}$ . The optimum value of the attenuation coefficient for the MEGP collimator was  $0.095\text{ cm}^{-1}$ , while that for the UHRFB collimator was significantly lower at  $0.07\text{ cm}^{-1}$ . Results for  $^{123}\text{I}$  images acquired with the MEGP collimator were similar to those observed with  $^{99m}\text{Tc}$  (optimum value =  $0.09\text{ cm}^{-1}$ ). However, those acquired with a UHRFB collimator showed that application of any type of attenuation correction resulted in an increase in the coefficient of variation of counts in the reconstructed image (Fig. 2B). This may be a consequence of septal penetration from the high-energy emissions of  $^{123}\text{I}$ . The effect of different attenuation coefficients on the measured striatal-to-occipital ratio was determined from  $^{123}\text{I}$  transaxial slices acquired with the MEGP and UHRFB collimators. For a true striatal-to-occipital ratio of 10, the measured values with the MEGP collimator were 4.86, 4.36 and 4.71 for  $\mu = 0.07, 0.12$  and  $0.15\text{ cm}^{-1}$ , respectively. For the UHRFB collimators, the

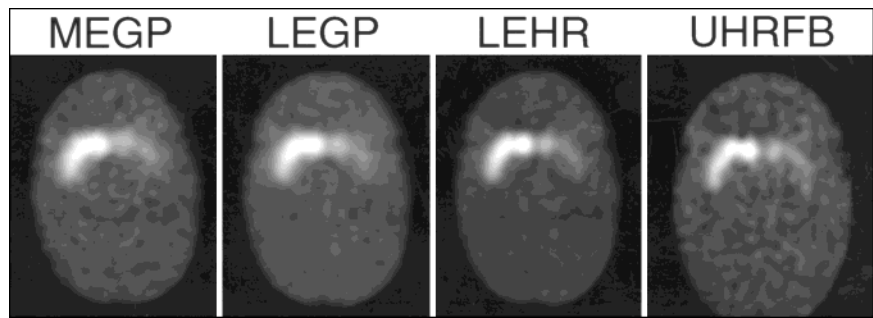


**FIGURE 3.** Representative transaxial slices through the midbrain section of the phantom demonstrating the impact of collimator resolution on image quality with  $^{99m}\text{Tc}$ . Images were acquired with the medium-energy (MEGP), low-energy general-purpose (LEGP), low-energy high-resolution (LEHR) and low-energy ultra-high resolution fanbeam (UHRFB) collimators.

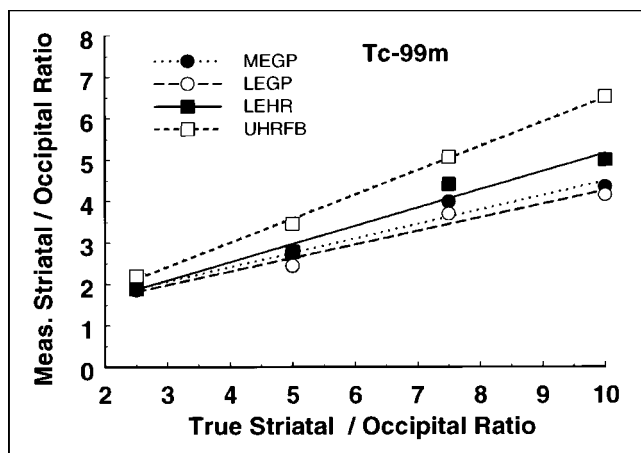
measured values were 4.84, 4.93 and 4.93 for  $\mu = 0.0, 0.12$  and  $0.15 \text{ cm}^{-1}$ , respectively.

Figure 3 illustrates the effects of different collimators on the resolution of the putamen and caudate in tomographic slices through the midbrain. There is a clear separation between the caudate and putamen in images acquired with the UHRFB and LEHR collimators, which is not apparent on the lower resolution images acquired with the LEGP and MEGP collimators.

Figure 4 plots the correlation between the true and measured striatal-to-occipital (S/O) ratios for the 4 collimators using  $^{99m}\text{Tc}$ . The caudate-to-occipital and putamen-to-occipital ratios were measured using  $4 \times 4$ -mm ROIs positioned on 1.76-cm thick transaxial images. The measured S/O ratios decreased inversely with collimator resolution. In all cases, the measured values underestimate the true ratios. Figure 5 plots the results from a similar experiment performed with  $^{123}\text{I}$  that used the range of activities shown in Table 2. With  $^{123}\text{I}$ , results obtained with the MEGP collimators were similar to those obtained with  $^{99m}\text{Tc}$ . However, results for  $^{123}\text{I}$  with the UHRFB collimators were significantly poorer than those seen with  $^{99m}\text{Tc}$  and were comparable to those obtained with the MEGP collimators. For the  $^{123}\text{I}$  acquisitions, the caudate-to-putamen ratio for each striatum also was determined. Each caudate and its corresponding putamen contained the same activity (true ratio = 1). Mean values for this ratio, were  $0.95 \pm 0.07$  (mean  $\pm$  SD) for the UHRFB collimator and  $0.93 \pm 0.05$  (mean  $\pm$  SD) for the MEGP collimator.

The results presented in Figures 4 and 5 were obtained on 1.76-cm thick transaxial slices. Figure 6 illustrates the effect of changes in slice thickness on the striatal-to-occipital ratio for the 4 collimators. Results were obtained from analysis of the caudate region in  $^{99m}\text{Tc}$  images with a true caudate-to-occipital ratio of 10:1. Increasing slice thickness reduced the apparent uptake in the striatum and the striatal-to-occipital ratio decreased inversely with increasing slice thickness. The differences in collimator resolution also were less pronounced with increasing slice thickness. A similar, but less pronounced, effect is seen with changes in the size of the ROIs. Figure 7 shows the decrease in the measured striatal-to-occipital ratio with increasing ROI size. With increase in the ROI size from  $1 \times 1$  to  $5 \times 5$  pixels, measured values of the S/O ratio decreased by 10–15% with the UHRFB and LEHR collimators, but only decreased by 5–7% with the LEGP and MEGP collimators.

The final variable that was examined in this study was the reconstruction filter. Figure 8 illustrates the effects of changes in the filter cutoff frequency and power (Butterworth filter) on the striatal-to-occipital ratio (measured over the caudate region; image data had a true caudate-to-occipital ratio of 10:1). Results were obtained using a  $4 \times 4$ -mm ROI on 1.76-cm transaxial slices obtained with  $^{99m}\text{Tc}$  on the LEHR collimator. While low cutoff values decreased the striatal-to-occipital ratio, cutoff values greater than  $0.4 \text{ cm}^{-1}$  had little effect on the ratio. A change in the order of the Butterworth filter from 5 to 10 did not alter the striatal-to-occipital ratio.



**FIGURE 4.** Correlation between true striatal-to-occipital ratio and measured striatal-to-occipital ratio for the 4 collimators. Results are based on analysis of 1.76-cm transaxial slices acquired with  $^{99m}\text{Tc}$  and an ROI of  $4 \times 4$ -mm dimensions.

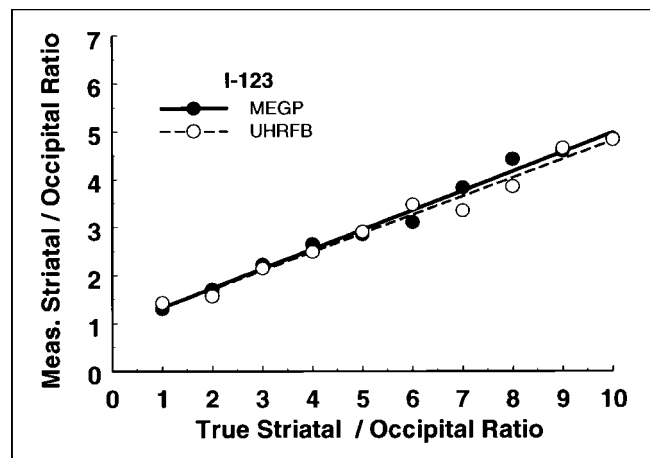


**FIGURE 5.** Correlation between true striatal-to-occipital ratio and measured striatal-to-occipital ratio for the MEGP and UHRFB collimators. Results are based on analysis of 1.76-cm transaxial slices acquired with  $^{123}\text{I}$  and an ROI of dimensions  $4 \times 4$  mm.

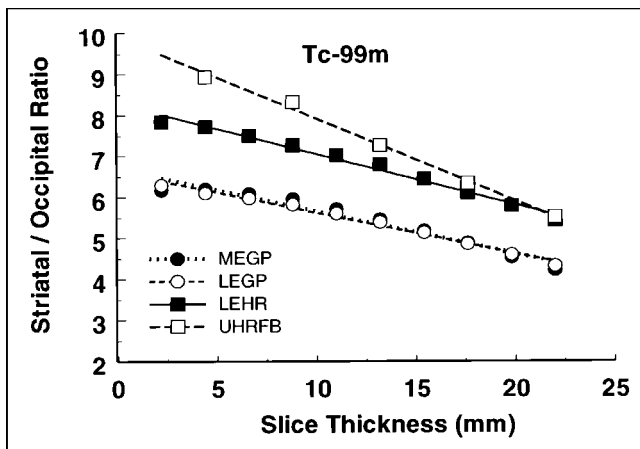


**FIGURE 6.** Relationship between measured striatal-to-occipital ratio and transaxial slice thickness for the 4 collimators. Results are based on analysis of transaxial slices acquired with  $^{99m}\text{Tc}$  and an ROI of  $4 \times 4$ -mm dimensions.

#### DISCUSSION

Over the last few years, numerous studies have reported on the usefulness of  $^{123}\text{I}$ - $\beta$ -CIT in the evaluation of patients with Parkinson's disease. In all these studies, a semiquantitative estimate of caudate, putamen or global striatal uptake of  $^{123}\text{I}$ - $\beta$ -CIT has been used reliably to detect abnormal uptake of  $^{123}\text{I}$ - $\beta$ -CIT in the dopamine receptors (3,5,6). In performing this semiquantitative analysis, a variety of different collimators, reconstruction filters, slice thickness and ROIs have been used. As a consequence intercomparison of striatal to nonstriatal uptake values between different laboratories has not been possible (9). While we recognize that differences in equipment may preclude accurate intercomparison of studies, a better understanding of the effect of various acquisition and processing parameters should allow laboratories to adjust for such differences and help minimize their impact on the reported range of values in patients and normal subjects.

One parameter that usually is not considered a factor in quantitative analysis is the attenuation coefficient used in data

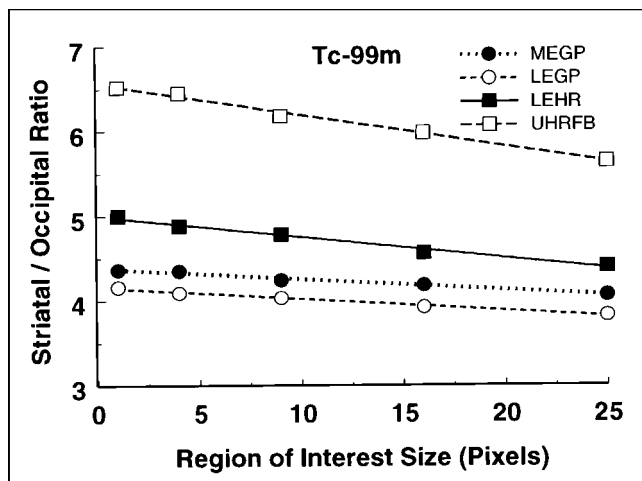


**FIGURE 7.** Relationship between measured striatal-to-occipital ratio and ROI size for the 4 collimators. Results are based on analysis of 1.76-cm transaxial slices acquired with  $^{99m}\text{Tc}$ .

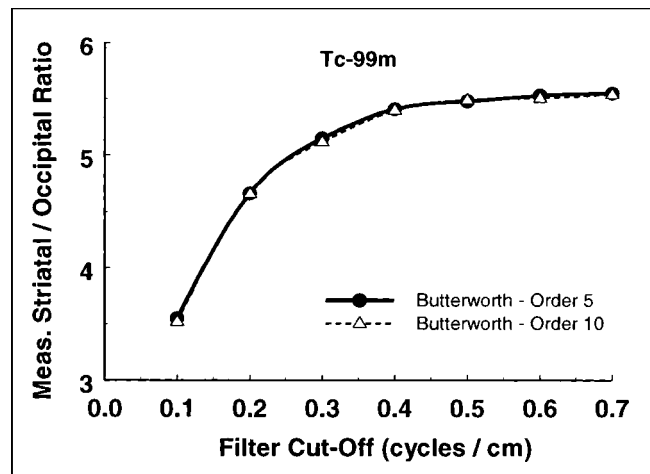


**FIGURE 8.** Relationship between measured striatal-to-occipital ratio and filter cutoff frequency for Butterworth filter with orders 5 and 10. Results are based on analysis of 1.76-cm transaxial slices acquired with  $^{99m}\text{Tc}$  and the low-energy high-resolution (LEHR) collimator with an ROI of  $4 \times 4$ -mm dimensions.

reconstruction. The attenuation coefficient for  $^{99m}\text{Tc}$  usually is assigned a value of  $0.12 \text{ cm}^{-1}$  in situations where a uniform attenuating material is present (13). However, the presence of bone in the skull has been shown to alter the optimum value for the attenuation coefficient  $\mu$  (10,14). We found an optimum value of  $\mu = 0.095 \text{ cm}^{-1}$  (Fig. 2A), comparable to that obtained by Kemp et al. (15) in a study of a human skull. This paradoxical decrease in the optimum value of  $\mu$  has been shown both theoretically and experimentally to be due to the effects of outer layers of attenuating material that are free of radioactivity (10). The use of a UHRFB collimator further reduces the optimum value of the attenuation coefficient ( $\mu = 0.07 \text{ cm}^{-1}$ ). This value is comparable to that obtained by Slodilka et al. (10) and is due to the increase in sensitivity with distance from the face of a fanbeam collimator (16). This results in an apparent increase in activity in the center of the brain with a fanbeam collimator compared to a parallel-hole collimator. This additional reduction in  $\mu$  will depend on the focal length of the UHRFB collimator with shorter focal length collimators showing the largest reduction. Changing the isotope from  $^{99m}\text{Tc}$  to  $^{123}\text{I}$  resulted in only a small change in the optimum value of  $\mu$  for the MEGP collimator, consistent with the small 19-keV difference in photopeak energies. However, with the UHRFB collimator, septal penetration from the high-energy emissions of  $^{123}\text{I}$  increased the apparent activity in the center of the brain. The application of attenuation correction only increased the variability of counts within the brain (Fig. 2B). Slight differences in the design of the UHRFB collimator (focal length, septal thickness, etc.), together with variations in the distribution of activity in the brain, will affect the degree and pattern of septal penetration. Hence, we would recommend that such collimators not be used in  $^{123}\text{I}$  studies of the brain since they offer no improvement in image contrast and are problematic with regard to attenuation correction. It is of interest to note that previous studies have used a range of collimator types (fanbeam, LEHR and MEGP) with  $^{123}\text{I}$  and have used an attenuation coefficient of  $\mu = 0.12 \text{ cm}^{-1}$  or  $\mu = 0.15 \text{ cm}^{-1}$  (3,5,6,12).

In this study we found that the use of an attenuation coefficient of  $\mu = 0.12 \text{ cm}^{-1}$  resulted in a 10% decrease in the apparent striatal-to-occipital ratio for  $^{123}\text{I}$  studies acquired with the MEGP collimator. At least to a small extent,  $\mu$  also will be dependent on window width and energy resolution of the system.

The effect of collimator resolution on the resolution of the caudate and putamen is shown in Figure 3. While differences in reconstructed image resolution could have been simulated by filtration, this would not reflect the distance-dependent effects of collimator resolution. As expected from the collimator specifications, the LEHR and UHRFB collimators provide improved visualization of the caudate and putamen compared to the lower resolution LEGP and MEGP collimators. In normal subjects the putamen and head of the caudate are relatively small structures with typical dimensions of 7–15 mm in the transaxial plane (17). These dimensions are comparable to the resolution of the 4 collimators evaluated in this study (Table 1). Partial volume effects become important for objects of dimensions less than twice system resolution and dominate when object size is equal to or less than system resolution (18). Given the size of the caudate and putamen, use of a high-resolution collimator is essential to obtain an accurate estimate of receptor uptake. Even so, measured striatal-to-occipital ratios are extremely sensitive to any parameter that effectively blurs the image data. Hence changes in collimator resolution (Fig. 4), slice thickness (Fig. 6) and ROI size (Fig. 7) all effect the ability to accurately measure the striatal-to-occipital ratio. This problem is compounded further by the presence of high-energy emissions from  $^{123}\text{I}$ . These emissions result in septal penetration with low-energy collimators and reduce image contrast. In this study, use of a low-resolution medium-energy collimator gave comparable results to those obtained with a high-resolution low-energy fanbeam collimator (Fig. 5). The relative trade-off between these 2 collimators likely will vary from system to system and will be highly dependent on the amount of septal penetration present in the  $^{123}\text{I}$  images.

Increased accuracy in determining relative caudate or putamen activity can be achieved by using the minimum slice thickness and the smallest ROIs (Figs. 6, 7). However, a decrease in slice thickness and ROI size may increase the variability in clinical studies, as small variations in the orientation of the transverse slices relative to the canto-meatal plane and minor changes in ROI position may alter parameters such as the caudate-to-occipital ratio, caudate-to-putamen ratio and measurement of left-to-right ratios. While filter cutoff frequency values greater than  $0.4 \text{ cm}^{-1}$  did not have a major impact on the measured striatal-to-occipital ratio, this analysis was performed on 1.76-cm thick transaxial slices. It is likely that the effects of filtration would be more pronounced on thinner slices and smaller ROIs (9).

## CONCLUSION

It is clear from Figures 4–8 that measurement of relative striatal uptake of  $^{123}\text{I}$ - $\beta$ -CIT in the brain is highly dependent on

a large number of acquisition and processing parameters. This dependence is due primarily to partial volume effects, as the caudate and putamen have dimensions comparable to system resolution. Partial volume effects combined with the averaging effects of increasing slice thickness and ROI size are the most significant factors affecting accurate measurement of relative striatal uptake of  $^{123}\text{I}$ - $\beta$ -CIT in the brain. Unfortunately, the increased resolution of low-energy high-resolution collimators, compared to a medium-energy collimator, is offset by the presence of septal penetration. These results would indicate that while each laboratory can readily establish its own normal range for  $^{123}\text{I}$ - $\beta$ -CIT uptake in the brain, intercomparison of data from different laboratories is likely to be difficult to achieve and will require phantom calibration studies to standardize such data.

## REFERENCES

- Mizukawa K, McGeer EG, McGeer PL. Autoradiographic study on dopamine uptake sites and their correlation with dopamine levels and their striata from patients with Parkinson disease, Alzheimer disease, and neurologically normal controls. *Mol Chem Neuropathol*. 1993; 18:133–144.
- Haberland N, Hetey L. Studies in postmortem dopamine uptake. II. Alterations of the synaptosomal catecholamine uptake in postmortem brain regions in schizophrenia. *J Neural Transm*. 1987; 68:303–313.
- Innis R, Baldwin R, Sybirska E, et al. Single photon emission computed tomography imaging of monoamine reuptake sites in primate brain with [ $^{123}\text{I}$ ]CIT. *Eur J Pharmacol*. 1991; 200:369–370.
- Neumeyer JL, Wang SY, Milius RA, et al. [ $^{123}\text{I}$ ]-2beta-carbomethoxy-3beta-(4-iodophenyl)tropane: high affinity SPECT radiotracer of monoamine reuptake sites in brain. *J Med Chem*. 1991; 34:3144–3146.
- Kuikka JT, Bergström KA, Vanninen E, et al. Initial experience with single-photon emission tomography using iodine-123-labelled 2beta-carbomethoxy-3beta-(4-iodophenyl)tropane in human brain. *Eur J Nucl Med*. 1993; 20:783–786.
- Seibyl JP, Marek KL, Quinlan D, et al. Decreased single-photon emission computed tomographic [ $^{123}\text{I}$ ]beta-CIT striatal uptake correlates with symptom severity in Parkinson's disease. *Ann Neurol*. 1995; 38:589–598.
- Ishikawa T, Dhawan V, Kazumata K, et al. Comparative nigrostriatal dopaminergic imaging with iodine-123-beta-CIT-FP/SPECT and fluorine-18-FDOPA/PET. *J Nucl Med*. 1996; 37:1760–1765.
- Booij J, Tissingh G, Winogrodzka A, et al. Practical benefit of [ $^{123}\text{I}$ ]FP-CIT SPET in the demonstration of the dopaminergic deficit in Parkinson's disease. *Eur J Nucl Med*. 1997; 24:68–71.
- Kuikka JT. Quantitation of neuroreceptors: a need to increase imaging resolution [Letter to Ed.]. *J Nucl Med*. 1996; 37:1911–1912.
- Stodilka RZ, Kemp BJ, Prato FS, Nicholson RL. Importance of bone attenuation in brain SPECT quantification. *J Nucl Med*. 1998; 39:190–197.
- Chang LT. A method for attenuation correction in radionuclide computed tomography. *IEEE Trans Nucl Sci*. 1978; NS-25:638–642.
- Brucke T, Kornhuber J, Angelberger P, et al. SPECT imaging of dopamine and serotonin transporters with [ $^{123}\text{I}$ ]beta-CIT. Binding kinetics in the human brain. *J Neural Transm*. 1993; 94:137–146.
- Harris CC, Greer KL, Jaszczak RJ, et al. Tc-99m attenuation coefficients in water-filled phantoms determined with a gamma camera. *Med Phys*. 1984; 11:681–685.
- Nicholson RL, Doherty M, Wilkins K, Prato FS. Paradoxical effect of the skull on attenuation correction requirements for brain SPECT [Abstract]. *J Nucl Med*. 1988; 29:1316.
- Kemp BJ, Prato FS, Dean GW, et al. Correction for attenuation in technetium-99m-HMPAO SPECT brain imaging. *J Nucl Med*. 1992; 33:1875–1880.
- Moore SC, Kouris K, Cullum I. Collimator design for single photon emission tomography. *Eur J Nucl Med*. 1992; 19:138–150.
- Jackson GD, Duncan JS. *MRI Neuroanatomy: A New Angle on the Brain*. New York, NY: Churchill Livingstone; 1996:74–90.
- Kojima A, Matsumoto M, Takahashi M, et al. Effect of spatial resolution on SPECT quantification values. *J Nucl Med*. 1989; 30:508–514.